Paper CIT06-0794

SIMULATION OF BUOYANT MASS TRANSPORT IN TURBULENT FLOWS IN POROUS MEDIA

Maximilian S. Mesquita
Departamento de Engenharia Mecânica
Universidade Federal do Espírito Santo
29060-900 – Vitória – E.S. - Brasil

Luzia A. Tofaneli
Marcelo J.S. De-Lemos[1]
Departamento de Energia - IEME
Instituto Tecnológico de Aeronáutica - ITA
12228-900 - São José dos Campos - SP – Brasil
[1] Corresponding author, delemos@ita.br.

Abstract. *This work presents derivations of mass transport for turbulent buoyancy flows in permeable structures. Equations are developed following two distinct procedures. The first method considers time averaging of the local instantaneous mass transport equation before the volume average operator is applied. The second methodology employs both averaging operators but in a reverse order. This work is intended to demonstrate that both approaches lead to equivalent equations when one takes into account both time fluctuations and spatial deviations of velocity and mass concentration. A modeled form for the final transport equation is presented where turbulent mass transfer with buoyancy is based on a macroscopic version of the* $k-\varepsilon$ *model.*

Keywords. *Numerical Method simulation of buoyancy, Porous Media, Turbulent Flow*

1. Introduction

The study of double-diffusive natural convection and buoyancy mass transport in porous media has many environmental and industrial applications, including grain storage and drying, petrochemical processes, oil and gas extraction, contaminant dispersion in underground water reservoirs, electrochemical processes, etc (Mamou et al., 1995, Mohamad & Bennacer, 2002, Goyeau et al., 1996, Nithiarasu et al., 1997, Mamou et al., 1998, Bennacet et al., 2001, Bennacet et al., 2003). In some specific applications, the fluid mixture may become turbulent and difficulties arise in the proper mathematical modeling of the transport processes under both temperature and concentration gradients.

Modeling of macroscopic transport for incompressible flows in rigid porous media has been based on the volume-average methodology for either heat Hsu & Cheng 1990 or mass transfer (Bear 1972, Bear & Bachmat, 1967, Whitaker , 1966, Whitaker , 1967). If time fluctuations of the flow properties are considered, in addition to spatial deviations, there are two possible methodologies to follow in order to obtain macroscopic equations: a) application of time-average operator followed by volume-averaging (Masuoka & Takatsu, 1996, Kuwahara et al., 1996, Kuwahara & Nakayama, 1998, Nakayama & Kuwahara, 1999), or b) use of volume-averaging before time-averaging is applied (Lee & Howell, 1987, Wang & Takle, 1995, Antohe & Lage, 1997, Getachewa et al., 2000). This work intends to present a set of macroscopic mass transport equations derived under the recently established double decomposition concept Pedras & de Lemos, 2000, 2001a, b and c, through which the connection between the two paths a) and b) above is unveiled. That methodology, initially developed for the flow variables, has been extended to heat transfer in porous media where both time fluctuations and spatial deviations were considered for velocity and temperature Rocamora & de Lemos, 2000. Buoyancy flows de Lemos & Braga, 2003 and mass transfer de Lemos & Mesquita, 2003 have also been investigated. Recently, a general classification of all proposed models for turbulent flow and heat transfer in porous media has been published de Lemos & Pedras, 2001. Here ,buoyancy mass transport flow in porous media is considered.

2. LOCAL INSTANTANEOUS TRANSPORT EQUATION

The steady-state microscopic instantaneous transport equations for an incompressible binary fluid mixture with constant properties are given by:

$$\nabla \cdot \mathbf{u} = 0 \qquad (1)$$

$$\rho \nabla \cdot (\mathbf{u}\mathbf{u}) = -\nabla p + \mu \nabla^2 \mathbf{u} + \rho\, \mathbf{g} \qquad (2)$$

$$\rho\nabla\cdot(\mathbf{u}\,m_\ell + \mathbf{J}_\ell) = \rho R_\ell \tag{3}$$

where $\mathbf{u}$ is the mass-averaged velocity of the mixture, $\mathbf{u} = \sum_\ell m_\ell \mathbf{u}_\ell$, $\mathbf{u}_\ell$ is the velocity of species ℓ, m_ℓ is the mass fraction of component ℓ, defined as $m_\ell = \rho_\ell / \rho$, ρ_ℓ is the mass density of species ℓ (mass of ℓ over total mixture volume), ρ is the bulk density of the mixture ($\rho = \sum_\ell \rho_\ell$), p is the pressure, μ is the fluid mixture viscosity, $\mathbf{g}$ is the gravity acceleration vector. The generation rate of species ℓ per unit of mixture mass is given in (3) by R_ℓ.

An alternative way of writing the mass transport equation is using the volumetric molar concentration C_ℓ (mol of ℓ over total mixture volume), the molar weight M_ℓ (g/mol of ℓ) and the molar generation/destruction rate R_ℓ^* (mol of ℓ /total mixture volume), giving:

$$M_\ell\nabla\cdot(\mathbf{u}\,C_\ell + \mathbf{J}_\ell) = M_\ell R_\ell^* \tag{4}$$

Further, the mass diffusion flux J_ℓ (mass of ℓ per unit area per unit time) in (3) or (4) is due to the velocity slip of species ℓ,

$$\mathbf{J} = \rho_\ell(\mathbf{u}_\ell - \mathbf{u}) = -\rho_\ell D_\ell \nabla m_\ell = -M_\ell D_\ell \nabla C_\ell \tag{5}$$

where D_ℓ is the diffusion coefficient of species ℓ into the mixture. The second equality in equation (5) is known as Fick's Law, which is a constitutive equation strictly valid for binary mixtures under the absence of any additional driving mechanisms for mass transfer Hsu & Cheng 1990. Therefore, no Soret or Dufour effects are here considered.

Rearranging (4) for an inert species, dividing it by M_ℓ and dropping the index ℓ for a simple binary mixture, one has,

$$\nabla\cdot(\mathbf{u}\,C) = \nabla\cdot(D\nabla C) \tag{6}$$

If one considers that the density in the last term of (2) varies with concentration only, for buoyancy driven flows, the Boussinesq hypothesis reads, after renaming this density ρ_C,

$$\rho_C \cong \rho[1-\beta_C(C-C_{ref})] \tag{7}$$

where the subscript ref indicates a reference value and β_C is the solute expansion coefficient, defined by,

$$\beta_C = -\frac{1}{\rho}\frac{\partial\rho}{\partial C}\bigg|_{p,T} \tag{8}$$

Equation (7) is an approximation of (8) and shows how density vary with concentration in the body force term of the momentum equation.

Further, substituting (7) into (2), one has,

$$\rho\nabla\cdot(\mathbf{uu}) = -\nabla p + \mu\nabla^2\mathbf{u} + \rho\,\mathbf{g}[1-\beta(C-C_{ref})] \tag{9}$$

Thus, the momentum equation becomes,

$$\rho\nabla\cdot(\mathbf{uu}) = -(\nabla p)^* + \mu\nabla^2\mathbf{u} - \rho\,\mathbf{g}[\beta_C(C-C_{ref})] \tag{10}$$

where $(\nabla p)^* = \nabla p - \rho\,\mathbf{g}$ is a modified pressure gradient.

As mentioned, there are, in principle, two ways that one can follow in order to treat turbulent flow in porous media. The first method applies a time average operator to the governing equation (3) before the volume average procedure is conducted. In the second approach, the order of application of the two average operators is reversed. Both techniques aim at derivation of a suitable macroscopic turbulent mass transport equation.

Volume averaging in a porous medium, described in detail in references (Slattery 1967, Whitaker , 1969, Gray & Lee, 1977), makes use of the concept of a Representative Elementary Volume (REV), over which local equations are integrated. After integration, detailed information within the volume is lost and, instead, overall properties referring to a REV are considered. In a similar manner, statistical analysis of turbulent flow leads to time mean properties. Transport equations for statistical values are considered in lieu of instantaneous information on the flow.

MACROSCOPIC TIME AVERAGED EQUATIONS FOR BUOYANCY FREE FLOWS

For non-buoyancy flows, macroscopic equations considering turbulence have been already derived in detail for momentum Pedras & de Lemos, 2001a, heat de Lemos & Braga, 2003, mass de Lemos & Mesquita, 2003 transfer and for this reason their derivation need not to be repeated here. They read:

Momentum transport

$$\rho\nabla\cdot\left(\frac{\bar{\mathbf{u}}_D\bar{\mathbf{u}}_D}{\phi}\right)=-\nabla(\phi\langle\bar{p}\rangle^i)+\mu\nabla^2\bar{\mathbf{u}}_D-\left[\frac{\mu\phi}{K}\bar{\mathbf{u}}_D+\frac{c_F\phi\rho|\bar{\mathbf{u}}_D|\bar{\mathbf{u}}_D}{\sqrt{K}}\right] \tag{11}$$

$$-\rho\phi\langle\overline{\mathbf{u}'\mathbf{u}'}\rangle^i=\mu_{t_\phi}2\langle\bar{\mathbf{D}}\rangle^v-\frac{2}{3}\phi\rho\langle k\rangle^i\mathbf{I} \tag{12}$$

$$\langle\bar{\mathbf{D}}\rangle^v=\frac{1}{2}\left[\nabla\left(\phi\langle\bar{\mathbf{u}}\rangle^i\right)+\left[\nabla\left(\phi\langle\bar{\mathbf{u}}\rangle^i\right)\right]^T\right] \tag{13}$$

$$\langle k\rangle^i=\langle\overline{\mathbf{u}'\cdot\mathbf{u}'}\rangle^i/2 \tag{14}$$

$$\mu_{t_\phi}=\rho c_\mu\frac{\langle k\rangle^{i\,2}}{\langle\varepsilon\rangle^i} \tag{15}$$

Mass transport

$$\nabla\cdot(\bar{\mathbf{u}}_D\langle\bar{C}\rangle^i)=\nabla\cdot\mathbf{D}_{eff}\cdot\nabla(\phi\langle\bar{C}\rangle^i) \tag{16}$$

$$\mathbf{D}_{eff}=\mathbf{D}_{disp}+\mathbf{D}_{diff}+\mathbf{D}_t+\mathbf{D}_{disp,t} \tag{17}$$

$$\mathbf{D}_{diff}=\langle D\rangle^i\mathbf{I}=\frac{1}{\rho}\frac{\mu_\phi}{Sc}\mathbf{I} \tag{18}$$

$$\mathbf{D}_t+\mathbf{D}_{disp,t}=\frac{1}{\rho}\frac{\mu_{t_\phi}}{Sc_t}\mathbf{I} \tag{19}$$

Coefficients $\mathbf{D}_{disp}$, $\mathbf{D}_t$ and $\mathbf{D}_{disp,t}$ in (17) appear due to the nonlinearity of the convection term.

MACROSCOPIC MASS DIFFUSION EFFECTS

If buoyancy effects due to mass concentration variation is included in the macroscopic equations, and additional flow drive is obtained. All mathematical details on including such effects in the turbulence model of Pedras & de Lemos, 2001a, are already available in de Lemos & Tofaneli, 2004, For that, only final equations are here presented, noting that the case herein investigated is a particular case of the general problem treated in de Lemos & Tofaneli, 2004.

Mean Flow

$$\rho\nabla\cdot\left(\frac{\bar{\mathbf{u}}_D\bar{\mathbf{u}}_D}{\phi}\right)=-\nabla(\phi\langle\bar{p}\rangle^i)+\mu\nabla^2\bar{\mathbf{u}}_D+\rho\,\mathbf{g}\phi[\beta_{C_\phi}\,(\langle\bar{C}\rangle^i-C_{ref})]-\left[\frac{\mu\phi}{K}\bar{\mathbf{u}}_D+\frac{c_F\phi\rho|\bar{\mathbf{u}}_D|\,\bar{\mathbf{u}}_D}{\sqrt{K}}\right] \tag{20}$$

Turbulent field

$$\rho\nabla.\left(\bar{\mathbf{u}}_D\langle k\rangle^i\right)=\nabla.\left[\left(\mu+\frac{\mu_{t_\phi}}{\sigma_k}\right)\nabla\left(\phi\langle k\rangle^i\right)\right]+P^i+G^i+G^i_{\beta_C}-\rho\phi\langle\varepsilon\rangle^i \tag{21}$$

$$\rho\nabla.\left(\bar{\mathbf{u}}_D\langle\varepsilon\rangle^i\right)=\nabla.\left[\left(\mu+\frac{\mu_{t_\phi}}{\sigma_\varepsilon}\right)\nabla\left(\phi\langle\varepsilon\rangle^i\right)\right]+\frac{\langle\varepsilon\rangle^i}{\langle k\rangle^i}\left[c_1P^i+c_2G^i+c_1c_3G^i_{\beta_C}-c_2\rho\phi\langle\varepsilon\rangle^i\right] \tag{22}$$

where c_1, c_2, c_3 and c_k are constants and the production terms have the following physical significance:

1. $P^i=-\rho\left\langle\overline{\mathbf{u}'\mathbf{u}'}\right\rangle^i:\nabla\bar{\mathbf{u}}_D$ is the production rate of $\langle k\rangle^i$ due to gradients of $\bar{\mathbf{u}}_D$;
2. $G^i=c_k\rho\dfrac{\phi\langle k\rangle^i|\bar{\mathbf{u}}_D|}{\sqrt{K}}$ is the generation rate of the intrinsic average of k due to the action of the porous matrix;
3. $G^i_{\beta C}=\beta^k_{C\phi}\phi\dfrac{\mu_{t_\phi}}{Sc_{t_\phi}}\mathbf{g}.\nabla\left\langle\bar{C}\right\rangle^i$ is the generation of $\langle k\rangle^i$ due to concentration gradients.

3. Results and Discussion

All results obtained during the development of this work are presented and discussed upon. Here, results are divided in two main sessions, involving each a certain domain configurations. First, in clear medium session, the cavities are assumed to be unobstructed so that no extra drag, either of viscous or form nature, are included in the momentum equations. In this session, both laminar flow and turbulent flow regimes are analyzed. Further, in the porous medium session, the cavities are completely filled with porous material and runs are made also for laminar and turbulent flow.

The problem considered is showed schematically in Fig.1 and refers to the two-dimensional flow in a clear (or a cavity filled with porous material) rectangular cavity of height H and width L , The Schmidt number is assumed to be a unity. The cavity is assumed to be of infinite depth the z-axis and a uniform mass concentration gradient is putting on the left side to opposing side (see Fig. 1a). Numerical computations were performed for square cavity used a stretched grid with 80 x 80 (CV).

The Figure 3 shows the constant-concentration lines and streamlines of a clear square cavity with the mass concentration gradient from the left to right side for solutal Rayleigh numbers ranging from 10^3 to 10^6. At $Ra_s=10^3$, the streamlines in Fig.3 indicate the existence of a single vortex with centre in the middle of the cavity. Corresponding constant-concentration lines (or isolines for mass concentration) Fig. 3a are almost parallel to the left side wall (position where are imposed the mass concentration value) indicating that most of the mass transfer is transferred by diffusion. The vortex is generated due the horizontal mass concentration gradient across the section. This gradient, $\partial C/\partial t$, is negative everywhere, inducing a clockwise oriented vorticity.

When the solutal Rayleigh number is increased to $Ra_s=10^4$ ($Ra_s=\dfrac{g\beta_c L^3\Delta C}{\nu}\cdot Sc$) , Fig. 3d, the central vortex is distorted into an elliptic shape and the effect of convection is more pronounced in the isoconcentrates, Fig. 3c. Mass concentration gradients are stronger near the vertical walls, but decrease in the center region. For $Ra_s=10^5$, Fig. 3f, the behavior continues. The central vortex is elongated and two secondary vortex appear inside it. The mass transfer by convection in the viscous boundary layer alters the mass concentration distribution to such an extent that the mass concentration gradients in the center of domain are close to zero. The Fig. 3e shows that, with this change in the sign of the source term, negative vorticity is induced within the domain. The also cause the development of secondary vortices in the core.

Increasing Ra_s to 10^6, Fig. 3h , causes the secondary vortices to move closer towards the walls and are convected further downstream. A third vortex appears in the domain rotating clockwise instead, reducing the shear stress between the order two vortice. In Fig. 3g , the mass transfer is now mostly by convection in the fast moving fluid near the walls.

Table 1 – Average Nusselt and Sherwood number for a clear square cavity for ranging from 10^3 to 10^6.

Nu / Sh				
	10^3	10^4	10^5	10^6
Barakos et al. (1994)	1.114	2.245	4.510	8.806
Markatos & Pericleous (1984)	1.108	2.201	4.430	8.754
Fusegi et al (1991)	1.105	2.302	4.646	9.012
De Vahl Davis (1983)	1.117	2.238	4.509	8.817
Braga and de Lemos (2002a)	1.127	2.249	4.575	8.918
Presents Results	1.128	2.512	4.578	8.921

Table 1 show the average Nusselt and Sherwood numbers for Ra_T and Ra_s ranging from 10^3 to 10^6. Its important notice that the values of average Nusselt numbers in the heat transfer are similarly that corresponds values to average Sherwood number. In this were used the analogy between heat and mass transfer to validate the results of the present work. The agreement of the literature results with the values obtained here are relatively good. From the engineering viewpoint, the most important parameter of the flow is the rate of heat (and mass concentration) transfer across the cavity. The Nusselt (Sherwood) number based on the hot wall (or more concentrate wall) at x = 0 is given by $Nu = \frac{hL}{k} \therefore Nu = \left(\frac{\partial T}{\partial x}\right)_{x=0} \frac{L}{T_H - T_C}$, $Sh = \frac{h_m L}{D_\ell} \therefore Sh = \left(\frac{\partial C}{\partial x}\right)_{x=0} \frac{L}{C_H - C_c}$, and its average value calculates as, $\overline{Nu} = \frac{1}{H}\int_0^H Nu \cdot dy$ and $\overline{Sh} = \frac{1}{H}\int_0^H Sh \cdot dy$ and $Da = \frac{K}{H^2}$.

Figure 4 shows the turbulent isoconcentrate and streamlines of a clear square cavity for Ra_s ranging from 10^8 to 10^{10}. The flow field at low solutal Ra values, not shown here, is similar to that obtained from laminar flow computations. However, the results are not exactly the same due to the inclusion of a turbulent viscosity. The similarity continues up to $Ra = 10^6$. For higher values of Ra_s, the model gives only turbulent solution. For $Ra_s = 10^8$, Fig. (4b), the central vortex disappears and the secondary vortices generated in the central core are convected further upstream and closer to the concentrates mass walls. The boundary layers on the concentrates mass walls are, at this moment, very thin. Increasing solutal Ra to 10^{10}, Fig. (4f) the central core is totally stratified. As solutal Ra further increases, the vortex system becomes progressively weaker and eventually, for solutal Rayleigh numbers greater than 10^{10}, it disappears completely. The velocities are high within the boundary layer and the flow in the central core is stratified.

The isotherms for solutal Ra = 10^8 and $Ra_s = 10^{10}$, Fig. (4a) and Fig. (4e), respectively, indicate an stratification of the flow outside the boundary layers and the mass concentration-profiles are almost horizontal for high values of Ra_s .

Figure 5 presents the turbulent isoconcentrate and streamlines of a square cavity filled with porous material, calculations were performed with 80x80 control volumes (CV) using a stretched grid. This part of the work tries to find for flow in porous media, a critical solutal Rayleigh, Ra_{scr}, for which simulations with the turbulence model departs from those considering laminar flow. Thus, the turbulence model is first switched off and the laminar branch of the solution is found. After that, the turbulence model is included so that the solution diverges from the laminar branch for Ra> Ra_{scr}. This separation of values as solutal Ra increases occurs at the so-called bifurcation point of the solution. As in the case of laminar flow in a square cavity filled with porous material, the parameters (Darcy number, Schmidt number, inertia parameter, mass diffusivity) are fixed. Figure (5b) shows the streamlines for $Ra_s = 10^6$. For solutal Ra up to 10^4 , not shown here, the solution with the turbulence model gives nearly the same values as those obtained with laminar flow computations. Even for solutal Ra up to 10^6 the flow pattern resembles the one for laminar solution, not shown here, but the mass transfer (like with heat transport) along the more mass concentrate wall is significantly increased. This point will be explained below. Figure (5a) shows the isoconcentrates for solutal Ra $= 10^6$. It is clearly seen from the Fig. (5a) the stratification of the flow with the increasing of the solutal Ra. Here also, as in the cases of streamlines mentioned above, the isoconcentrate shown in Figure (5a) also are similar to those calculated with the laminar flow model.

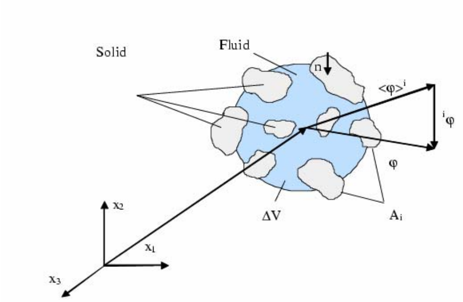

Figure 1 – Representative Elementary Volume, ΔV .

(a) (b)
Figure 2 – Square cavity (a) and the grid (b) for laminar and turbulent flow simulation.

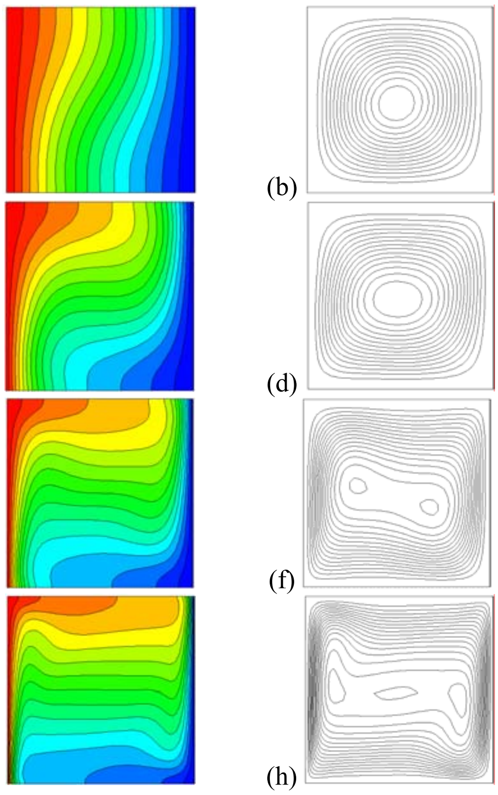

(a) (b) (c) (d) (e) (f) (g) (h)

Figure 3 – Laminar Constant-concentration lines and Streamlines for clear square cavity with mass concentration gradients from left side to right side for Ra ranging from 10^3 to 10^6 .

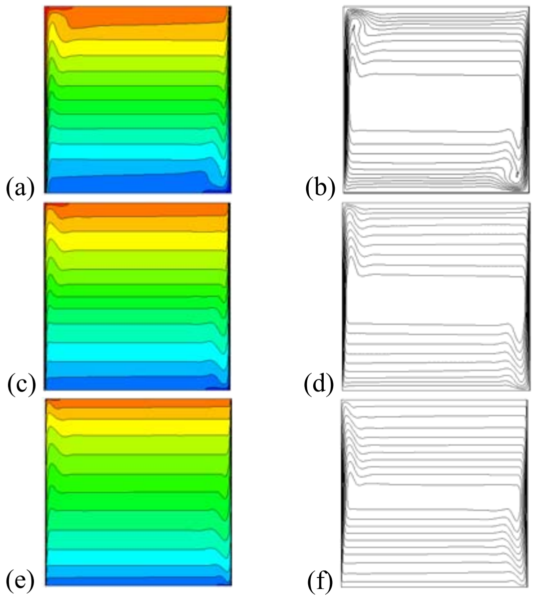

Figure 4 – Turbulent Constant-concentration lines and streamlines for clear square cavity with mass concentrations gradients from left side to right side for Ra ranging from 10^8 to 10^{10}.

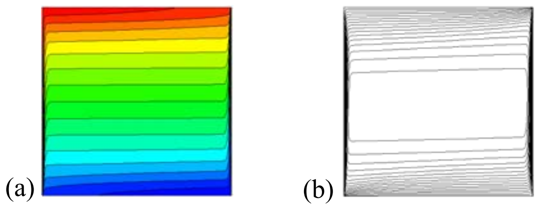

Figure 5 – Constant-concentration lines and streamlines for turbulent flow in a square cavity filled with porous material for $Ra = 10^6$ with $Dp = 1mm$ and $\phi = 0.80$.

4. Acknowledgement

The authors are thankful to CNPq, CAPES and FAPESP, Brazil, for their financial support during the course of this research.

5. References list

Antohe, B. V. & Lage, J. L., 1997. A general two-equation macroscopic turbulence model for incompressible flow in porous media, International Journal Heat Mass Transfer, vol.40, n.13, pp. 3013 - 3024.

Bear, J., 1972. Dynamics of Fluids in Porous Media, Dover, New York.

Bear, J. & Bachmat, Y., 1967. A generalized theory on hydrodynamic dispersion in porous media, I.A.S.H. Symp. Artificial Recharge and Management of Aquifers, Haifa, Israel, P.N. 72, pp. 7-16, I.A.S.H..

Bennacer, R., Tobbal, A., Beji, H. & Vasseur, P., 2001. Double diffusive convection in a vertical enclosure filled with anisotropic porous media, International Journal of Thermal Sciences, vol. 40, n. 1, pp.30-41.

Bennacer, R., Beji, H. & Mohamad, A. A., 2003. Double diffusive convection in a vertical enclosure inserted with two saturated porous layers confining a fluid layer, International Journal of Thermal Sciences, vol. 42, n. 2, pp.141-151.

de Lemos, M.J.S. & Braga, E.J., 2003. Modeling of turbulent natural convection in porous media, International Communications Heat Mass Transfer, vol. 30 n. 5, pp. 615 - 624.

de Lemos, M.J.S. & Mesquita, M.S., 2003. Turbulent mass transport in saturated rigid porous media, International Communications Heat Mass Transfer, vol. 30, pp. 105 - 113.

de Lemos, M.J.S. & Pedras, M.H.J., 2001. Recent mathematical models for turbulent flow in saturated rigid porous media, Journal of Fluids Engineering, vol.123, n. 4, pp. 935 - 940.

de Lemos, M.J.S. & Tofaneli, L.A., 2004. Modeling of double diffusive turbulent natural convection in porous media, International Journal Heat Mass Transfer, vol. 47, pp. 4233-4241.

de Lemos, M.J.S. & Rocamora Jr., F.D., 2002. Turbulent transport modeling for heated flow in rigid porous media, Proceedings of the Twelfth International Heat Transfer Conference, pp. 791-795.

Getachewa, D., Minkowycz, W.J. & Lage, J.L, 2000. A modified form of the kappa-epsilon model for turbulent flows of an incompressible fluid in porous media, International Journal Heat Mass Transfer, vol.43, n. 16, pp. 2909 - 2915.

Goyeau, B., Songbe, J.P. & Gobin, D., 1996. Numerical study of double-diffusive natural convection in a porous cavity using the Darcy-Brinkman formulation, International Journal of Heat and Mass Transfer, vol.39, n. 7, pp.1363-1378.

Gray, W.G. & Lee, P.C.Y., 1977. On the theorems for local volume averaging of multiphase system, Int. J. Multiphase Flow, vol.3, pp.333 -340.

Hsu, C.T. & Cheng, P., 1990. Thermal dispersion in a porous medium, International Journal Heat Mass Transfer, vol.33, pp.1587-1597.

Kuwahara, F., Nakayama, A. & Koyama, H., 1996. A numerical study of thermal dispersion in porous media, Journal of Heat Transfer, vol.118, pp.756.

Kuwahara, F. & Nakayama, A., 1998. Numerical modeling of non-Darcy convective flow in a porous medium, Heat Transfer , Proc. 11th Int. Heat Transf. Conf., Kyongyu, Korea, vol. 4, pp. 411-416, Taylor & Francis Washington, D.C..

Lee, K. & Howell, J.R., 1987. Forced convective and radiative transfer within a highly porous layer exposed to a turbulent external flow field, Proceedings of the 1987 ASME-JSME Thermal Engineering Joint Conf., Honolulu, Hawaii, vol. 2, 377-386, ASME, New York, N.Y..

Mamou, M., Vasseur, P. & Bilgen, E., 1995. Multiple solutions for double-diffusive convection in a vertical porous enclosure, International Journal of Heat and Mass Transfer, vol. 38, n. 10, pp. 1787-1798.

Mamou, M., Hasnaoui, M., Amahmid, A. & Vasseur, P., 1998. Stability analysis of double diffusive convection in a vertical brinkman porous enclosure, International Communications in Heat and Mass Transfer, vol. 25, n. 4, pp. 491-500.

Masuoka, T. & Takatsu, Y., 1996. Turbulence model for flow through porous media, International Journal Heat Mass Transfer, vol.39, n. 13, pp. 2803 - 2809.

Mohamad, A. A. & Bennacer, R., 2002. Double diffusion natural convection in an enclosure filled with saturated porous medium subjected to cross gradients; stably stratified fluid, International Journal of Heat and Mass Transfer, vol.45, n. 18, pp. 3725-3740.

Nakayama & Kuwahara, F., 1999. A macroscopic turbulence model for flow in a porous medium, Journal of Fluids Engineering, vol.121, pp. 427 - 433.

Nithiarasu, P., Sundararajan, T., & Seetharamu, K.N., 1997. Double-diffusive natural convection in a fluid saturated porous cavity with a freely convecting wall, International Communications in Heat and Mass Transfer, vol. 24, n. 8, pp.1121-1130.

Pedras, M.H.J & de Lemos, M.J.S., 2000. On the definition of turbulent kinetic energy for flow in porous media, Internernational Communications Heat and Mass Transfer, vol. 27 n. 2, pp. 211 - 220.

Pedras, M.H.J. & de Lemos, M.J.S., 2001. Macroscopic turbulence modeling for incompressible flow through undeformable porous media, International Journal Heat and Mass Transfer, vol. 44, n. 6, pp.1081 - 1093.

Pedras, M.H.J. & de Lemos, M.J.S., 2001. Simulation of turbulent flow in porous media using a spatially periodic array and a lowre two-equation closure, Numerical Heat Transfer - Part A Applications, vol. 39, n. 1, pp.35.

Pedras, M.H.J. & de Lemos, M.J.S., 2001. On the mathematical description and simulation of turbulent flow in a porous medium formed by an array of elliptic rods, Journal of Fluids Engineering, vol. 23, n. 4, pp. 941 - 947.

Rocamora Jr., F.D. & de Lemos, M.J.S., 2000. Analysis of convective heat transfer for turbulent flow in saturated porous media, International Communications Heat and Mass Transfer, vol. 27, n. 6, pp.825 - 834.

Slattery, J.C., 1967. Flow of viscoelastic fluids through porous media, A.I.Ch.E. J., 13, pp. 1066 - 1071.

Trevisan, O. & Bejan, A., 1985. Natural convection with combined heat and mass transfer buoyancy effects in a porous medium, International Journal Heat and Mass Transfer, vol.28, pp.1597-1611.

Wang, H. & Takle, E.S., 1995. Boundary-layer flow and turbulence near porous obstacles .1. derivation of a general equation set for a porous-medium, Boundary Layer Meteorology, vol.74, pp.73 - 78.

Whitaker, S., 1967. Diffusion and dispersion in porous media, J. Amer. Inst. Chem. Eng, vol.3, n. 13, pp. 420.

Whitaker, S., 1969. Advances in theory of fluid motion in porous media, Indust. Eng. Chem., vol.61, pp. 14 - 28.

Whitaker, S., 1966. Equations of motion in porous media, Chem. Eng. Sci., 21, pp.91.